

Proteomic, Functional, and Domain-Based Analysis of In Vivo 14-3-3 Binding Proteins Involved in Cytoskeletal Regulation and Cellular Organization

Jing Jin,^{1,6} F. Donelson Smith,^{2,6} Chris Stark,¹ Clark D. Wells,¹ James P. Fawcett,¹ Sarang Kulkarni,¹ Pavel Metalnikov,¹ Paul O'Donnell,¹ Paul Taylor,³ Lorne Taylor,³ Alexandre Zougman,³ James R. Woodgett,⁴ Lorene K. Langeberg,² John D. Scott,² and Tony Pawson^{1,5,*}

¹Samuel Lunenfeld Research Institute
Mount Sinai Hospital
600 University Avenue
Toronto, Ontario M5G 1X5
Canada

²Howard Hughes Medical Institute
Vollum Institute
Oregon Health & Science University
Portland, Oregon 97239

³Protana Analytical Services
MDS Proteomics
251 Attwell Drive
Toronto, Ontario M9W 7H4
Canada

⁴Ontario Cancer Institute
610 University Avenue
Toronto, Ontario M5G 2M9
Canada

⁵Department of Medical Genetics and Microbiology
University of Toronto
Toronto, Ontario M5S 1A8
Canada

Summary

Background: 14-3-3 proteins are abundant and conserved polypeptides that mediate the cellular effects of basophilic protein kinases through their ability to bind specific peptide motifs phosphorylated on serine or threonine.

Results: We have used mass spectrometry to analyze proteins that associate with 14-3-3 isoforms in HEK293 cells. This identified 170 unique 14-3-3-associated proteins, which show only modest overlap with previous 14-3-3 binding partners isolated by affinity chromatography. To explore this large set of proteins, we developed a domain-based hierarchical clustering technique that distinguishes structurally and functionally related subsets of 14-3-3 target proteins. This analysis revealed a large group of 14-3-3 binding partners that regulate cytoskeletal architecture. Inhibition of 14-3-3 phosphoprotein recognition in vivo indicates the general importance of such interactions in cellular morphology and membrane dynamics. Using tandem proteomic and biochemical approaches, we identify a phospho-dependent 14-3-3 binding site on the A kinase anchoring protein (AKAP)-Lbc, a guanine nucleotide exchange factor

(GEF) for the Rho GTPase. 14-3-3 binding to AKAP-Lbc, induced by PKA, suppresses Rho activation in vivo.

Conclusion: 14-3-3 proteins can potentially engage around 0.6% of the human proteome. Domain-based clustering has identified specific subsets of 14-3-3 targets, including numerous proteins involved in the dynamic control of cell architecture. This notion has been validated by the broad inhibition of 14-3-3 phosphorylation-dependent binding in vivo and by the specific analysis of AKAP-Lbc, a RhoGEF that is controlled by its interaction with 14-3-3.

Introduction

Many aspects of dynamic cellular behavior are regulated by reversible protein phosphorylation [1]. Protein kinases frequently exert their biological effects by creating docking sites for interaction domains, which selectively recognize phosphorylated motifs in their binding partners [2]. 14-3-3 proteins were the first polypeptides shown to have phosphoserine/threonine (pSer/Thr) binding properties [3]. Structural analysis has shown that each 14-3-3 protomer folds into an α -helical structure with a conserved binding groove that accommodates pSer/Thr-containing sites [4, 5], typically generated by basophilic kinases such as cAMP-dependent protein kinase (PKA) and protein kinase B (PKB) [6, 7]. Accordingly, two optimal 14-3-3 phosphopeptide ligands with the consensus sequences RSXpSXP and RXY/FXpSXP (where X is any amino acid) have been defined with degenerate peptide libraries [4]. However, several 14-3-3 binding proteins interact through phosphorylated motifs that diverge from this consensus [8], and in some cases 14-3-3 proteins can also recognize unmodified proteins [9–11].

14-3-3 proteins are abundant and are encoded by seven mammalian genes (α/β , ϵ , η , γ , π/θ , ζ/δ , and σ) that can be traced through vertebrates, plants, and yeast [10]. They typically form stable homo- and heterodimers as a result of reciprocal contacts between their N-terminal α helices. These dimers therefore present a rather rigid structure with two distinct, but closely apposed, phosphopeptide binding sites and potentially serve as adaptors to juxtapose two separate phosphoproteins [4]. However, a more common role may be as allosteric regulators that stabilize their binding partners in a particular conformation. Thus, a 14-3-3 dimer appears to clamp serotonin N-acetyltransferase in an enzymatically active configuration [5]. 14-3-3 proteins can also regulate the formation of multi-protein complexes by binding to one component of such an assembly and restricting its access to other partners. The binding of 14-3-3 to phosphorylated BAD to block its pro-apoptotic association with Bcl-XL is an example [12]. Alternatively, 14-3-3 proteins can restrict the subcellular location of their ligands, typified by retention of the 14-3-3-associated FoxO transcription factor FKHR in the cytoplasm [13]. Consistent with this view, analysis of individual 14-3-3

*Correspondence: pawson@mshri.on.ca

⁶These two authors made equal contributions.

binding partners in cells, as well as large-scale identification of potential 14-3-3 ligands by *in vitro* affinity chromatography, has revealed a number of diverse polypeptides that can potentially associate with 14-3-3 proteins [14, 15].

Here, we have used a direct proteomic analysis of 14-3-3 γ binding proteins in HEK293 (human embryonic kidney) cells. Our results identify *in vivo* 14-3-3 binding partners that are associated with a remarkable range of cellular activities but show only partial overlap with previous proteomic analysis of *in vitro* 14-3-3 targets. To understand this large volume of information, we have developed a domain-based clustering approach that identifies and visualizes multiple subsets of 14-3-3 binding proteins. A significant group of 14-3-3 binding proteins distinguished through this approach is involved in control of the cytoskeleton. We have employed a cell-based approach to analyze the general role of 14-3-3 proteins in controlling cell morphology. We also describe a specific cytoskeletal regulator, AKAP-Lbc, that was identified in tandem proteomic and biochemical screens for 14-3-3 binding partners that are also scaffolds and substrates for basophilic kinases. Activation of the Rho GTPase by AKAP-Lbc is regulated by 14-3-3 in a cAMP-dependent manner.

Results and Discussion

Isolation of 14-3-3 Protein Complexes from HEK293 Cells

HEK293 cells were transiently transfected with plasmids encoding Flag-tagged human α/β , ζ/δ , γ , or τ/θ isoforms of 14-3-3. 14-3-3 complexes were isolated with immobilized anti-Flag antibodies, and the associated proteins were released upon incubation with a Flag peptide. These protein mixtures were separated by gel electrophoresis, stained with colloidal Coomassie blue dye (Figure S1 in the Supplemental data available with this article online), excised, and digested with trypsin. The resulting peptides were analyzed by LC-tandem mass spectrometry (MS/MS) and assigned to specific proteins with the Mascot search engine. As shown in Table S1, many proteins were identified in association with each isoform (α/β , 71; γ , 127; τ/θ , 19; and ζ/δ , 26), with Flag-14-3-3 γ yielding the largest number of interactions. To avoid problems of overexpression associated with transient transfection, we isolated a HEK293 cell line that stably expresses Flag-14-3-3 γ at a level similar to that of endogenous isoforms (data not shown) for subsequent analysis.

The most prominent Flag-14-3-3 γ binding partners identified by LC-MS/MS in this stably expressing cell line were the seven endogenous 14-3-3 isoforms (Figure S2), consistent with the ability of 14-3-3 proteins to form homo- and heterodimers [16]. The immunoprecipitation approach can therefore capture proteins that interact not only with ectopic Flag-14-3-3 γ , through either direct or indirect association, but also with endogenous 14-3-3 isoforms. Several observations suggest that the 14-3-3-associated proteins detected in this screen are biologically relevant. In addition to a large set of novel 14-3-3 partners, we isolated a significant fraction of proteins

known to associate with 14-3-3s (see notes in Table 1). Furthermore, control experiments indicated that anti-Flag precipitates from parental HEK293 cells had little background. As a positive control, Flag-14-3-3 γ immunoprecipitates were eluted with a GST fusion containing a 20 amino acid peptide (R18) that binds to the 14-3-3 phosphopeptide recognition pocket and displaces associated phosphoproteins [17, 18]. The proteins eluted by Flag or R18 peptides were largely identical, except that both bait and endogenous 14-3-3 proteins were absent from the R18 eluate, as anticipated (Figure S2). This observation, taken with the finding that treatment of cells with Calyculin-A (an inhibitor of the PP1 and PP2A phosphatases) increased the overall binding of cellular proteins to 14-3-3 γ (data not shown), indicates that the majority of proteins are associated with 14-3-3 through pSer/Thr recognition.

Domain-Based Cluster Analysis Identifies Related Sets of 14-3-3-Associated Proteins

Peptides identified by MS/MS analysis were assigned to specific protein GI (GenInfo Identifier, National Center for Biotechnology Information [NCBI]) numbers; these were filtered, and redundancies were removed primarily based on their LocusID numbers (see Supplemental Experimental Procedures for details) (Tables 1 and S3). In total, we identified 170 unique 14-3-3 γ -associated proteins implicated in a broad range of cellular activities; only a few of these proteins are potentially nonspecific (proteins also identified in control β TrCP immunoprecipitates are marked in Table 1). All identified proteins were characterized according to GO (Gene Ontology Consortium, <http://www.geneontology.org/>) categories that define their biological and molecular functions [19], as indicated in Figure 1 and Table 1. The largest group of 14-3-3-interacting proteins is involved in cellular communication and signal transduction (45%). Significant numbers of 14-3-3 targets are also implicated in cellular organization (10%), energy and metabolism (3%), and nucleic acid synthesis and processing (15%), among others. A schematic summary of the 14-3-3-associated proteins that fall into each of these functional categories, with further annotation of their molecular function, is presented in Figure 1. This figure also identifies a significant proportion (approximately 60%) of proteins that contain a 14-3-3 mode 1 binding consensus [20] (for details, also see Table S2).

This analysis indicates that 14-3-3 interacting proteins potentially amount to approximately 0.6% of the human proteome, suggesting pleiotropic functions for 14-3-3 proteins in cells. We have taken advantage of the modular nature of cell regulatory proteins to obtain an overarching view of 14-3-3-mediated interactions and to explore whether this large number of proteins can be further grouped into functional or structural subsets. To this end, we employed a hierarchical clustering approach, commonly used to analyze and visualize microarray data, by grouping genes according to similarities in their expression patterns [21]. For our purposes, we identified interaction and catalytic domains present in each 14-3-3 binding protein, as predicted by SMART (Simple Modular Architecture Research Tool) and Pfam

Table 1. 14-3-3γ Interacting Proteins

Protein GI	Protein Name / Gene Symbol	Domain	Notes
Cellular Communication and Signal Transduction			
Adaptor Molecule			
12655023	14-3-3 alpha-beta	14-3-3	Endogenous 14-3-3s bind to bait flag-14-3-3γ through reciprocal dimerization
1168198	14-3-3 epsilon	14-3-3	
1345593	14-3-3 eta	14-3-3	
6018858	14-3-3 gamma	14-3-3	
998953	14-3-3 sigma	14-3-3	
112690	14-3-3 tau-theta	14-3-3	
14278220	14-3-3 zeta-delta	14-3-3	
9257199	Bai1-associated protein 2 isoform 2 / BAIAP2 / IRSp53	SH3	Binds to Mena, cdc42, WAVE, Rac, regulates filopodia [1] [2]
4454524	Similar to insulin receptor substrate BAP2 / LOC55971	coiled coil, SH3	Homologous to BAP2/IRSp53
7305303	Nck associated protein 1/NCKAP1 / NAP125		Complex with WAVE1 and PIR121 [3] [4]
5616320	p53 inducible protein/PIR121 / CYFIP2		Complex with WAVE1 and NCKAP/NAP125 [3] [4]
19923303	growth factor receptor-bound protein 10 / GRB10	RA, PH, SH2	
4102707	NUMB-R protein, numb homolog / NUMBL	PTB, NumbF	Involved in asymmetric cell division, inhibitor of notch [5]
52880195	Myosin phosphatase and Rho interacting protein 3/M-RIP	PH, F-actin binding protein	Binds to RhoA and regulates actin cytoskeletal organization [6]
23398532	yes associated protein / YAP	WW, coiled coil	14-3-3 binding attenuates p73 mediated cell death [7]
29731	c-cbl protein / CBL	Cbl_N1-3, Ring	14-3-3 binding [8]
14537854	insulin receptor substrate 2 / IRS-2	PH, PTB	14-3-3 binds to IRS-1 [9]
4504733	insulin receptor substrate 4 / IRS-4	PH, PTB	
8037915	PAR3	PDZ	Complex with Par6, αPKC and 14-3-3 [10]
17433253	SH3 adaptor protein SPIN90	SH3, Coeffector of mDia Rho GTPase	Nck interacting, regulates actin polymerization and cell adhesion turnover [11]
11527203	sporulation-induced transcript 4-associated protein / SAPLb	SAPs (phosphatase associated protein)	
7661968	entrophin / epsin 4	ENTH	Proteins with ENTH domain participate in clathrin-mediated endocytosis [12]
22538473	Eps15 binding protein / epsin 2	ENTH	
1401126	TAK1 binding protein / TAB1	PP2C (phosphatase)	Binds to TAK1 and controls SAPK/p38, IKK activation [13] [14]
Adhesion Molecule			
3152861	p120 catenin / CTNND1	coiled coil, ARM repeats	Polarity protein [15]
Cell Cycle Control Protein			
12655137	NUDEL / NDE1	Nude_C	14-3-3ε k/o phenotype resembles Miller-Dieker Syndrome and relates to NUDEL binding [16]
Protein Kinase			
10944890	Wee1 protein / WEE1*	kinase	14-3-3 binds to and regulates Wee1 activity which acts on cdc2-cyclinB [17]
4502803	CHK1 / CHEK1	kinase	Checkpoint kinase, binds to 14-3-3, activates Wee1 kinase [18]
66762	raf-1	RBD (ras binding), C1, kinase	Binds to 14-3-3 [19]
4502193	v-raf / Araf-1 / ARAF1	RBD (ras binding), C1, kinase	
23346414	MARK3 / Par1A / CTAK1	kinase, UBA, KA (kinase associate)	Phosphorylates Par3 and induces its binding to 14-3-3 [20]
8923922	MAP / microtubule affinity-regulating kinase1/ MARK1	kinase, UBA, KA (kinase associate)	
9845487	MARK2 / Par1B	kinase, UBA, KA (kinase associate)	
21735556	MARPK2 / MEKK2	BP1, kinase	Binds to 14-3-3 [21]
1313646	MEK kinase 3 / MAP2K3 / MEKK3	PEB/Prox and Bem1p, kinase	Stress activated protein kinase known to bind to 14-3-3 via ser166 phosphorylation [22]
12711660	protein kinase lysine deficient 1 / WNK1 / PRKWINK1	kinase, coiled coil	Mutations in WNK kinases are linked to human inherited hypertension. [23]
18314669	PKC iota / PRKCI	PB1, C1, kinase, PKC-C-term Domain	An atypical PKC that regulates cell polarity
11493219	PKC-like 2 / PRK2 / PKNgamma	HR1 repeats, C2, kinase, PKC-C-term	Binds to and is activated by a small GTPase Rac [24]
18765750	dual-specificity tyrosine-phosphorylation regulated kinase 1A/DYRK1A	kinase	Overexpression causes mental retardation and motor anomalies similar to Down syndrome [25]
19172411	mixed-lineage kinase-related kinase MRK-alpha / ZAK	kinase, coiled coil, SAM	Cell cycle regulation
13276655	CaMKK alpha protein / CAMKK1	kinase domain	Regulates axonal extension and growth cone motility [26]
29791476	p21-activated kinase 4 / PAK1	PBD (p21Rho-binding domain), kinase	PAK complexes with Pix and GIT in modulating cdc42 activation [27]
12585288	p21-activated kinase 4 / PAK4	PBD (p21Rho-binding domain), kinase	
21542571	PCTAIRE protein kinase 2 / PCTK2	kinase	PCTAIRE1 is phosphorylated by PKA and associated with 14-3-3 [28]
Phosphatase			
495192	PP2A B alpha subunit	WD40	PP2A associates with and regulates αPKC in tight junctions[29]
4505317	protein phosphatase 1 regulatory subunit / PPP1R12A	ANK repeats, coiled coil	Associated with 14-3-3 [30]
34328899	Protein tyrosine phosphatase, non-receptor type 14 / PTPN14	B41, PTPc	
17455719	KIAA1157 protein/ras homolog gene family, member C like 1	PP2C phosphatase domain	
41149877	AF-1 specific protein phosphatase	Spry, HECT	
8925284	phosphatidylinositol polyphosphate 5-phosphatase type IV / INPP5E	IPPc (inositol phosphatase)	
G protein: GTPase: GTPase activating protein: Guanine nucleotide exchange factor: small GTPases effector protein			
17646186	protein kinase A anchoring protein H31, Lbc / AKAP-Lbc/ AKAP13	C1, RhoGEF, PH	Scaffolding protein, see text for details
19744759	GEF-H1 / ARHGEF2 / Lfc	coiled coil, C1, RhoGEF, PH	Binds to 14-3-3 [31]
4505573	Rho GEF 7 isoform a / beta Pix / ARHGEF7	SH3, RhoGEF, PH, coiled coil	Functions with GIT and PAK, regulates focal adhesions [27]
22027525	Rac-cdc42 GEF6 / alpha Pix / ARHGEF6	CH, SH3, Rho-GEF, PH, coiled coil	
34530826	FYVE, RhoGEF and PH domain containing 6 / FGD6	RhoGEF, PH, FYVE, PH	
15077826	rap guanine nucleotide exchange factor / RAPGEF6	CNMP, RasGEFN, PDZ, RA, RasGEF	Homologous to the WRP/srGAP family RhoGAPs that bind to WAVE1 and Robo
25535897	KIAA0456 protein/formin binding protein 2/FNBP2	FCH, coiled coil, RhoGAP, SH3	
93977541	Rho-GAP 10 / RhoGAP21 / ARHGAP21	PDZ, PH, RhoGAP	
25535899	Rac GAP-1	coiled coil, C1, RhoGAP	
42659261	DKFZP434C212 protein / KIAA1521 protein / DKFZP434C212	RasGAP, VPS9 (vacuolar sorting protein)	
4758808	Ras protein activator like 2 isoform 1/ RASAL2	PH, C2, RasGAP, coiled coil	
10938010	tuberous sclerosis 2 isoform 3 / TSC2 / tuberin	tuberin, RapGAP	Complex with TSC1, phosphorylation by PKB/AKT induces 14-3-3 binding [32]
4691726	ArfGAP GIT1	ARFGAP, ANK, GIT	Functions with Pix and PAK, regulates focal adhesions
21237786	ArfGAP GIT2	ARFGAP, ANK	
28461223	guanine nucleotide binding protein (beta-polypeptide 2-like 1)/GNB2L1	WD40 repeats	
3153873	putative G-binding protein CRFG	GTPase	
2598196	Regulator of G protein signaling 12 / RGS12	RGS, RBD, GoLoco	Family members RGS3 and RGS7 bind to 14-3-3 [33]
27469680	Rabaptin-5, RAB GTPase binding effector protein 1 / RABEP1	Rabaptin, coiled coil, V_ATPase_1	Role in endocytosis, apical recycling [34]
13377897	Rab11 interacting protein / Rab-FIP / RIPI1	C2	Regulator of endocytosis through Rab11
20068811	Rab-coupling protein / RCP	C2	Rab effector protein homologous to Rab-FIP
27530920	ERC1 / ELKS delta / Rab6-interacting protein / CAST	coiled coil	ELKS-Rab6-interacting protein-CAST (ERC) binds to RIM protein at presynaptic active zones [35]
Un-subclassified			
25044789	mucoepidermoid susceptibility protein / MECT1		Translocation in mucoepidermoid carcinoma, regulator of notch signaling [36]
40068509	dedicator of cytokinesis 11 / DOCK11	PH	
19923493	phosphoinositide 3-phosphate-binding protein-2 / PEPP2	WW, PH, coiled coil	
5031729	WD-repeat protein (putative G protein) / HAN11	WD40 repeats	
21955172	LL5 beta / LLSB	coiled coil, PH	PI(3,4,5)P sensor that also binds to cytoskeletal adaptor, gamma-flaminin. [37]
Energy and Metabolism			
Superoxide dismutase; Phosphotransferase; Dehydrogenase; Synthetase; ATPase			
21429608	SOD copper chaperone / CCS	HMA, sodcu	
33350932	dynein, cytoplasmic, heavy polypeptide 1 / DNCH1	ATPase	
12643333	6PF-2-K / PFKFB2	6PF2K, PGAM	Phosphorylated by PKB/Akt and binds to 14-3-3 [43]
625366	succinate dehydrogenase (ubiquinone)	FAD-Binding_2, Succ_DH_Flav_C	
18105007	carbamoyl phosphate synthetase 2 / CPS1	CarA, CarB, PyrC, PyrB	
Protein Synthesis, Processing and Protein Fate			
15421129	elongation factor 1a / EEF1A1*	GTP_EFTU, GTP_EFTU_D2, GTP_EFTU_D3	
23491733	ribosomal protein S2*	ribosomal S5	
6996447	Hsp60 / HSPD1*	Chaperonin GroEL	
18043726	hsp70 / HSPA8*	HSP70	
20070125	prolyl 4-hydroxylase, beta subunit; v-erb-a homolog 2-like / P4HB	Thioredo	
4090929	chaperonin-containing TCP-1 beta / CCT2	TCP1	
20070220	SKB1*	Skb	
7453575	protein arginine N-methyltransferase 1-variant 2 / HRMT1L2	mythyltransferase	
32698744	ubiquitin specific protease 37 / USP37	UIM repeats	

(continued)

Table 1. Continued

Protein GI	Protein Name / Gene Symbol	Domain	Note
Nucleic Acid Synthesis and Processing			
Cell Cycle Control Protein			
4506749	ribonucleotide reductase M1 subunit / RRM1	ATP_cone, ribonuc_red_lgc	
DNA Binding Protein			
13446225	zinc finger protein	BTB, zinc_finger_C2H2_repeats	
1232079	hulkM5 / hulkM5	MCM1, minichromosome maintenance	
2687853	RAD50 homologue hRAD50	coiled coil, Rad50_Zn_Hook	DNA repair
Deacetylase			
13259524	histone deacetylase 7A / HDAC7A	HisDeac1	14-3-3 binding mediates nuclear exclusion of some histone deacetylases [44]
5174481	histone deacetylase 4 / HDAC4	HisDeac1	
20981706	CTP synthase / CTPS	GATase	
Ribonucleoprotein			
13111793	hNRP-M / HNRPM*		
12803583	HNRPA3 protein / HNRPA3*	RRM (RNA recognition motif)	
RNA Binding Protein			
2231592	mRNA associated protein, mrnp41 / REA1	WD40 repeats	RNA binding protein
8979741	poly-A binding protein 1 / PABPC1	RRM repeats, polyA	
2832596	dj434p1.3, DEAD/H box polypeptide	DEXDc, HELICc	
6002955	cleavage and polyadenylation specificity factor 3 / CPSF3	LactamaseB	
7440064	fus-like protein*	RRM, ZnF_RBZ	
7657383	non-Pou domain-containing octamer binding protein	RRM repeats, coiled coil	
4885225	Ewing sarcoma breakpoint region 1 / EWSR1	RRM	
27436873	NF2 histone linker PHD ring helicase / SHPRH	DEXDc, Ring, HELICc	
Transcription Factor; Transcription Regulatory Protein			
6175059	transcription factor E3 / TFE3	HLH	
431254	PAX3 protein-forkhead transcription factor, PAX3-FKHR	PAX, FH	FoxO class of transcription factors - 14-3-3 binding mediates nuclear exclusion [45]
4503739	forkhead box O3A / FOXO3A	FH	FoxO class of transcription factors - 14-3-3 binding mediates nuclear exclusion
7228111	transcription factor/SMI1/decapping enzyme hDec1b / HSA275986	DCP1	Smad 4 interacting [46] [47]
33860140	Apoptosis stimulating of p53 protein 2 / 53BP2 / TP53BP2	Coiled coil, ANK, SH3	Also Bcl2-binding protein [48]
17225574	LIM domain only 7, FBX20 / LMO7	CH,coiled coil, PDZ,LIM	
4507353	TBP-associated factor 15 / TAF15*	RRM, Zinc_finger domain	
4502603	chromobox homolog 4 / CBX4	Chromo	
Cellular Organization			
Cell Junction Protein			
1871540	plakophilin 2 / PKP2	ARM repeats	Phosphorylation by C-TAK1 promotes binding to 14-3-3 [38]
6174575	myeloid/lymphoid or mixed-lineage leukemia / AF6 / Afadin / MLLT4	RA, FHA, DII, PDZ	
Cytoskeletal Protein			
13277909	Tubulin / Tubb5	Tubulin, Tubulin_C	
2337952	actin-binding double-zinc-finger protein / ABLM1	LIM, coiled coil, VHP (vacuolar sorting)	Actin binding and axon guidance [39]
7705373	epithelial protein lost in neoplasm beta / EPLIN	LIM	Regulates actin dynamics [40]
11496982	supervillin isoform 2 / SVIL	GEL repeats, VHP	Membrane-associated F-actin binding protein p205
4507195	spectrin, beta / SPTBN1	CH, Spectrin repeats, PH	
4505983	PTPRF interacting protein alpha 1 isoform b / Liprin-a / Syd-2 / LIPRIN	Coiled coil, SAM domain repeats	LAR-interacting protein, also associated with ERC/CAST [40]
25989336	tumor-associated microtubule-associated protein / TMAP		
34536177	E-MAP-115-95, microtubule associated protein 7	HELP, WD40 repeats	
13124319	kinesin heavy chain isoform 5 / KIF5C	KISc, coiled coil	
5031831	kinesin 2	TPR repeats	14-3-3 binding to phospho-ser575 [41]
21735548	centrosomal protein 2/centrosomal Nek2-associated protein 1/C-Nap1	coiled coil, V_ATPase_1	
Structural Protein			
439434	integral nuclear envelope inner membrane protein / LBR	Tudor, transmembrane domain	
4758012	clathrin heavy chain 1 / CLTC	Clathrin, Propel repeats, CLH repeats	
4503745	filamin 1 (actin-binding protein-280) / FLNA	CH, filamin repeats	
4507693	tuberous sclerosis 1 / TSC1 / Hamartin	Hamartin, coiled coil	Binds to TSC2 which complexes with 14-3-3 [42]
Storage and Transportation			
7705837	potassium channel tetramerisation domain containing 3	K+ channel tetramerisation domain	
22760412	unnamed protein, phosphate carrier protein / PHC	mito_carr repeats	
Unclassified			
20070384	hypothetical protein / MGC5352	GpmB, Fructose-2,6-bisphosphatase	Fructose-2,6-bisphosphatase homology domain similar to that of 6PF-2-K
16359152	AKT1S1 protein / AKT1S1		
12053233	unnamed protein product / kinesin like / KLC2	TPR repeat domain	
11360247	unknown, DKFZp761H229.1/kinesin like 8	TPR repeat domain	
2224623	Nedd4 binding protein 3 / N4BP3	coiled coil	
15214282	SAPK interacting protein 1 / MAPKAP1		
13569874	FIP1-like 1/ rearranged in hypereosinophilia	FIP1 (Polyadenylation factor I complex)	FIP1L1-POGRalpha fusion found in myeloproliferative disease [49]
10834652	PP203	BTB, WD40 repeats	
21748574	FLJ00364 protein / transducer of regulated CREB 3/ TORC3		
28436730	multiple coiled-coil GABABR1-binding protein / MARLIN1	Coiled coil	
7243023	KIAA1321 protein / 82-kD FMRP Interacting Protein / 182-FIP		
20988634	chromosome 12 ORF2 / C12orf2	RA (ras association), coiled coil	
4589526	KIAA0941 protein	C2	
13874435	cerebral protein-10 / FLJ10579		
10437164	FJL21128	CDC9(DNA ligase), YjeF_N	
24901318	FLJ10211 protein	SAM	
5699443	KIAA1053 protein / sterile alpha motif domain containing 4 / SAMD4	SAM	
7022115	unnamed protein product / FLJ10211		
27477498	unnamed protein product		
13960126	Hypothetical protein / MGC4126	Leucine-rich repeats (LRR), CH	
17433099	band 4.1-like protein 3 / EPB41L3	Band_4.1, SAB	Binds to 14-3-3 isoforms, Spectrin and Actin Binding [50]
7657562	SH3-domain binding protein 4 / SH3BP4	SH3	
7652198	TBC1 domain family member 4	PTB,TBC, coiled coil	
7652142	KARP-1-binding protein / KAB	PHA	Interacts with Ku autoantigen/KARP-1, component of DNAPK complex [51]
4502175	apical protein of Xenopus-like / APXL	PDZ, coiled coil	Localized to apical membrane and implicated in amiloride-sensitive sodium channel activity [52]
22052926	KIAA1960	coiled coil, Bar	Shares homology region with APXL
3882183	KIAA0731 / likely ortholog of mouse Ia related protein / LARP	LA, DM15 repeats	
5699653	KIAA1108 / TBC1 domain family, member 1/ TBC1D1	TBC, Domain in Tre-2, BUB2p, Cdc16p	
27529909	KIAA1448 protein / KIF1B	kinesin, FHA	
7513045	KIAA0627		Homologous to KIAA0627
7513102	KIAA0622		
27481856	similar to KIAA1999 protein		
32598702	HECT domain containing 1/ HECTD1	ANK, HECTc	
37540639	RIKEN 9030227G01	Fry-like	
20141917	Protein KIAA0062	DEXDc, HELICc	
31418642	Retinoic acid induced 14 / RAI14	ANK repeats, coiled coil	

References are shown in Supplementary References
* proteins also co-immunoprecipitate with control protein, Flag-beta-TrCP

14-3-3γ-associated proteins identified by LC-MS/MS are listed according to their unique LocusLink gene symbols. Each protein is described by its various names (NCBI protein accession descriptions) and domain composition (obtained from SMART [http://glyan.embl-heidelberg.de/] and Pfam [http://pfam.wustl.edu/]), with domains listed in order from N to C terminus. Proteins are grouped according to their GO biological and molecular functions (annotated in NCBI LocusLink and the Human Protein Reference Database [www.hprd.org] for the proteins or close relatives). The color code for GO biological functions is given in Figure 1. References in notes are provided in the Supplemental Data.

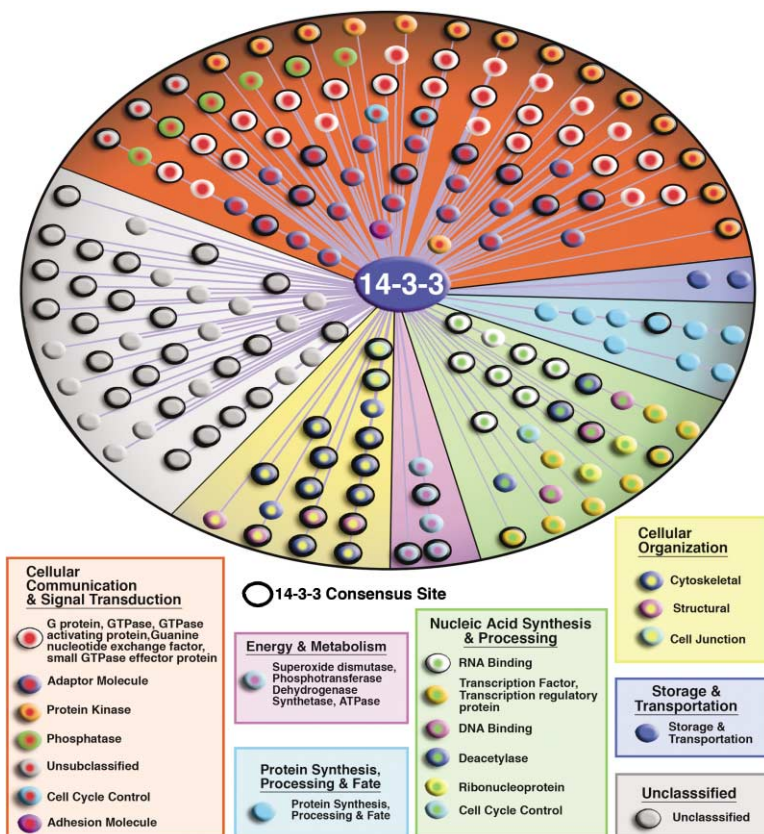


Figure 1. Functional Grouping of 14-3-3 Interacting Proteins

Each 14-3-3-interacting protein (Table 1) is illustrated as a node (individual circle). Proteins are grouped according to their GO biological functions, such as “cellular communication and signal transduction” (color-coded background in each segment). Each separate protein is color coded for its GO molecular properties, such as “protein kinase.” Proteins with potential mode 1 14-3-3 binding motifs are distinguished by solid black circles around the relevant nodes.

(Protein Family Database) (see Supplemental Experimental Procedures and Table S3 for details). We then used a statistical algorithm based on the average-linkage method to establish a similarity metric that relates proteins based on the correlation coefficient of their domains, and vice versa. This unbiased procedure yields a two-dimensional hierarchical clustering matrix, which groups proteins that have similar binding or enzymatic domains and may therefore participate in related biological processes (Figures 2 and S3–S8).

In this map (Figure 2), individual proteins are shown on the horizontal axis and are colored according to their functional GO annotation, with a dendrogram (generated by TreeView programming [21]) that reflects the phylogenetic order of proteins and domains in the cluster map. Proteins with a closely related set of modular domains, such as protein kinases or PH domain-containing proteins, will cluster together in the horizontal dimension. The vertical axis shows the presence or absence of individual modular domains in a given protein (for example, PDZ, SH3, or RhoGEF domains). Consequently, the map reflects the relatedness of 14-3-3 binding proteins according to their domain structure (a detailed list of proteins with full domain annotation is given in Table S3).

Strikingly, this approach yields a number of prominent clusters, of which three are shown in more detail (see the red, green, and blue boxes in Figures 2 and 3). The red cluster contains primarily protein serine/threonine kinases, which also possess a number of non-catalytic modules that direct their interactions with regulators or substrates (i.e., the PB1 heterodimerization domain and

GTPase binding domains) [22–27]. The green cluster is focused on proteins implicated in membrane association and actin regulation or as scaffolds for signaling pathways. A feature of these proteins is the presence of PH, RhoGEF (DH), RhoGAP, SH3, PDZ, or PTB domains, among others. Proteins in the blue cluster have varied functions, with a common theme being trafficking and the dynamic organization of larger subcellular structures. For example, Liprin- α and Erc1b regulate vesicle docking at presynaptic active zones, Rabaptin-5, Rab-FIP, and RCP regulate membrane recycling, and kinesin and dynein govern motor activity, whereas 53BP2, hsRAD50, and C-NAP1 control DNA and chromosome stability [28, 29]. A frequent element of these proteins is the presence of contractile domains (i.e., Myosin tail 1 and MAD domains).

This analysis shows that a significant fraction of 14-3-3-associated proteins can be grouped into subsets with related domains and, by inference, with related functions. We have exploited this approach to compare 14-3-3-interacting proteins obtained with different techniques. Two recent proteomic studies have employed the *in vitro* binding of human HeLa cell proteins to immobilized yeast Bmh1/Bmh2 14-3-3 proteins [14] or 14-3-3- ζ [15] to identify associated proteins. We have compared the results from these studies with proteins identified here that coprecipitate from HEK293 cells with Flag-tagged 14-3-3 isoforms. To this end, we combined the data obtained from “*in vitro*” binding into a single, non-redundant group, and similarly amalgamated the interacting proteins we identified from stable and tran-

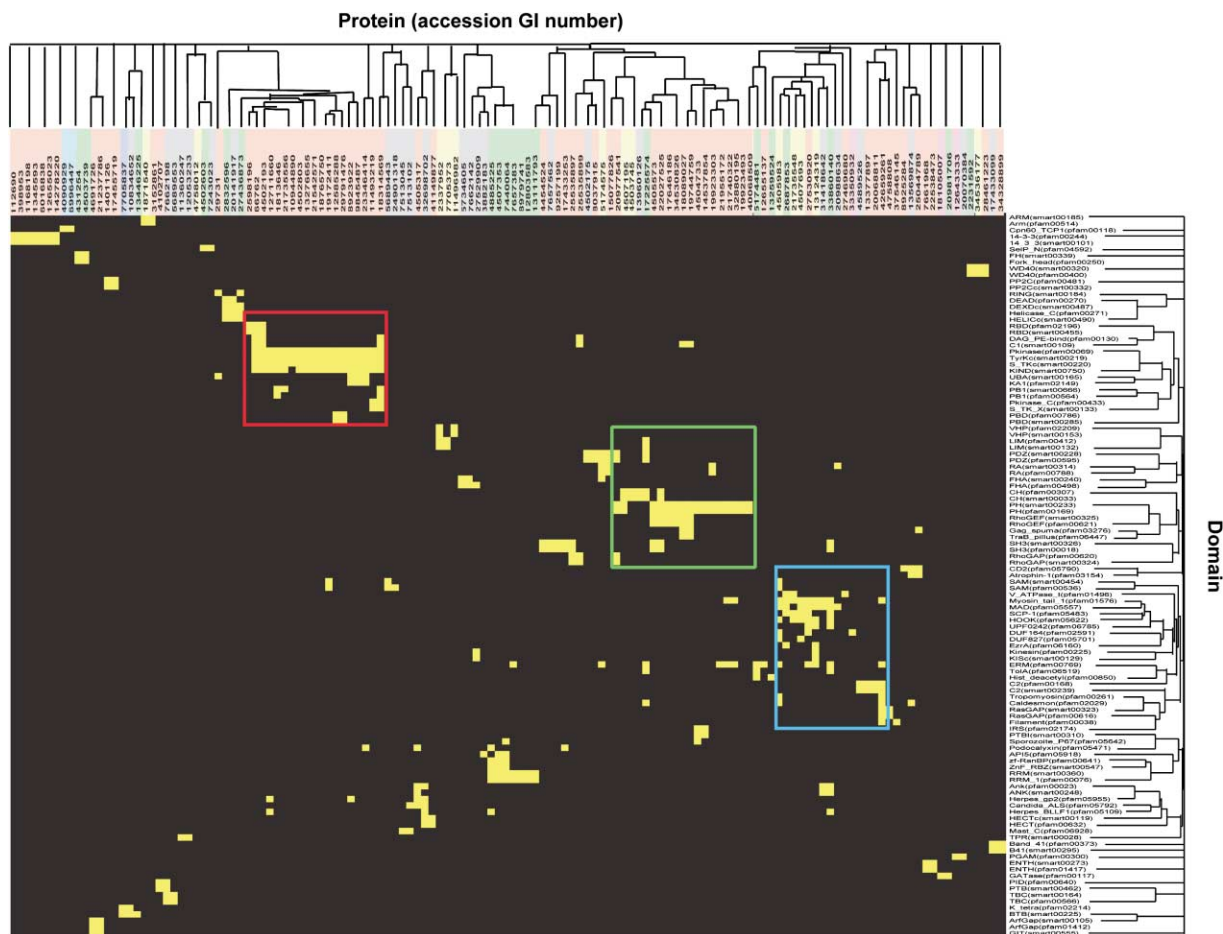


Figure 2. Comprehensive Analysis of 14-3-3 Binding Proteins by Domain-Based Hierarchical Clustering

SMART and Pfam definitions were used for analyzing sequences from each 14-3-3 binding protein for their domain composition. Proteins were then ranked by hierarchical clustering based on their domain content. In the resulting map, proteins (identified by GI numbers and color coded for their GO biological function as in Figure 1) are arrayed on the x axis, and domains from SMART and Pfam are on the y axis. A yellow square indicates the presence of a given domain within a specific protein sequence. The ordering of proteins and domains along the two axes depends on the hierarchical clustering process; the relationships of proteins and domains are also defined by phylogenetic trees, as shown. Three prominent clusters are indicated by red, green, and blue boxes. Magnified versions of these three clusters are shown in Figure 3, with the proteins identified by specific names (see Supplemental Experimental Procedures for details).

sient transfections into an “in vivo” set. When these in vivo or in vitro datasets were individually subjected to domain-based clustering, they yielded distinct patterns (Figure S4). Consistent with this, there is only a partial overlap (approximately 26%) between the 14-3-3 binding proteins identified by in vivo and in vitro techniques, potentially because of differences in the purification procedures or the use of different cells (Figure 4; for details, see Supplemental Experimental Procedures).

To obtain a more comprehensive view, the “in vitro” and “in vivo” groups were pooled and then clustered by domains (Figure 4). Interestingly, this integrated dataset shows that 14-3-3 binding proteins identified by coprecipitation (this study; colored yellow) or in vitro affinity purification [14, 15] (colored blue) frequently cocluster in specific groups (i.e., Figure 4, boxes B, D, and F–I). For example, specific coclusters contain protein kinases (box H), cytoskeletal regulators, polarity proteins, and signaling scaffolds (box G), as well as proteins involved in trafficking, dynamics, and contractile functions (box

F) (see Figure S5–S8 for expanded versions of all clusters). The coclustering of 14-3-3 binding proteins identified through different approaches argues that the physiological processes represented by each group are broad targets for control by 14-3-3 proteins. Of particular interest, box G (Figures S5–S8) represents an expanded version of the green cluster in Figure 2 and contains a diverse series of proteins involved in cytoskeletal regulation, control of Rho, Rab, and Rap family GTPases, membrane signaling, trafficking, focal adhesions, and cell polarity. This grouping of proteins that control cell architecture and adhesion demonstrates the utility of domain-based clustering in identifying functionally interconnected polypeptides within a large dataset.

14-3-3 Binding Proteins Have Diverse Functions

The clustering analysis of in vivo 14-3-3 binding proteins suggests that 14-3-3 proteins can impinge simultaneously on multiple facets of cellular behavior, consistent with the functional annotations in Figure 1 and Table 1.

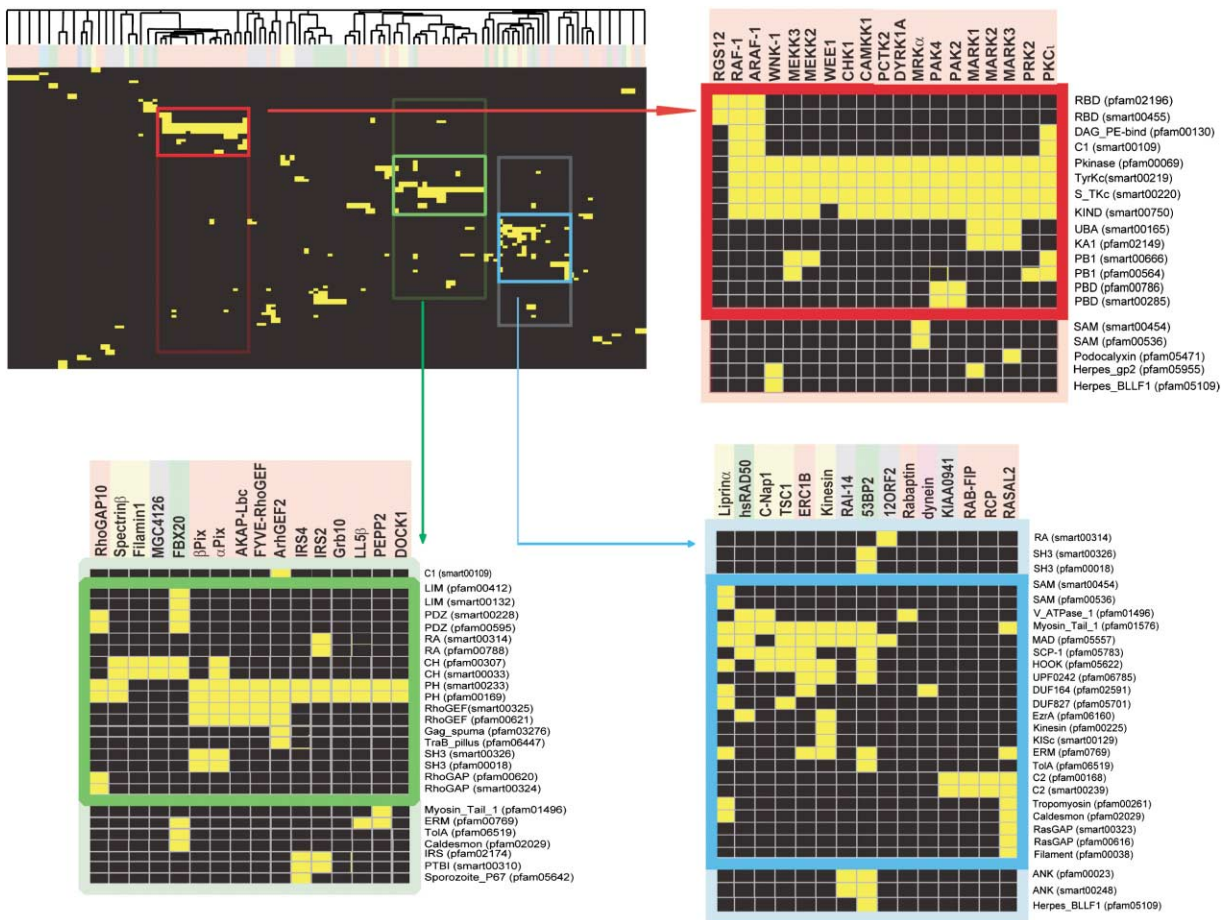


Figure 3. Magnified Versions of the Three Prominent Clusters Shown in Figure 2

In signal transduction, we identified 18 protein Ser/Thr kinases and 24 molecular adaptors, as well as several serine/threonine phosphatase components and a phosphatidylinositol (PI) 5'-phosphatase [30], suggesting that 14-3-3 proteins regulate the balance of cellular protein and lipid phosphorylation through association with both kinases and phosphatases. Of interest, we obtained multiple members of specific protein kinase families (MARK, PAK, and Ste11-related MAPKKK) as well as kinases with novel or poorly studied 14-3-3 binding properties (i.e., WNK1, PKN, DYRK1A, MRK α , and CaMKK). Among these are disease-implicated gene products, including the Arg-directed kinase DYRK1A implicated in Down's Syndrome [31, 32] as well as WNK1, which is mutated in pseudohyperaldosteronism type II, resulting in hypertension [33].

Novel 14-3-3-associated proteins are also involved in both heterotrimeric and monomeric G protein-dependent signaling (Table 1). Among these are proteins that directly regulate G $_{i\alpha 2}$ and 14 guanine nucleotide exchange factors (GEF) and GTPase activating proteins (GAP) for Rho, Arf, and Rap GTPases. In addition, we have found small-GTPase effector proteins, including Rab GTPase targets, and Rho family-dependent protein kinases such as PRK2/PKN γ and PAK1/4. These data argue for significant control of small-GTPase pathways,

as well as heterotrimeric G protein signaling, by phospho-dependent 14-3-3 interactions.

14-3-3s bind metabolic proteins [8], notably phosphorylated 6-phosphofructo-2-kinase (6PF-2-K), which contains an N-terminal kinase domain and a C-terminal phosphatase domain (PGAM). In addition to 6PF-2-K, we found a novel 14-3-3-associated protein, MGC5352 (listed under "unclassified" in Table 1), which shares homology with the 6PF-2-K's PGAM domain but lacks the kinase domain. It will be of interest to test whether this protein participates in glycolytic regulation. In this vein, a significant number of 14-3-3-associated proteins are poorly characterized (unclassified) but have known interaction domains indicative of signaling functions (i.e., FHA, SH3, PDZ, SAM, TPR, ANK, WD40, BTB, and RA) and frequently possess consensus mode 1 14-3-3 recognition sites (Figure 1 and details in Table S2).

14-3-3-Associated Proteins in Regulation of the Cytoskeleton and Cell Polarity

As noted, numerous proteins identified in this screen are involved in regulation of the actin cytoskeleton, polarity, focal adhesions, and endocytosis (summarized in Figure 5A). Cell polarity and asymmetric cell division are controlled by a conserved network of interacting proteins, identified genetically in *C. elegans* as the products of

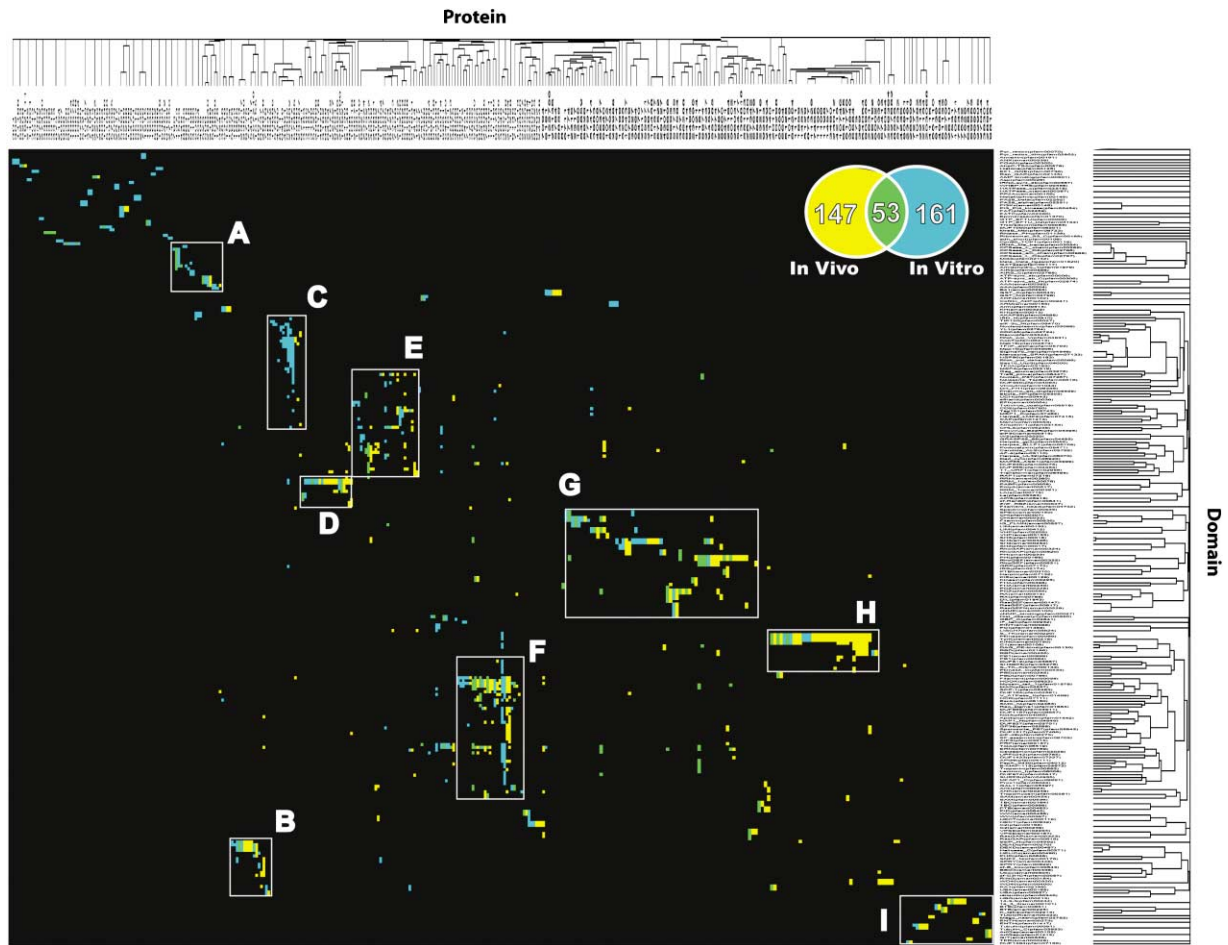


Figure 4. Comparison of In Vivo and In Vitro 14-3-3 Binding Proteins by Hierarchical Domain Clustering
Domain-based hierarchical clustering was applied to a combined dataset of 14-3-3-associated proteins, including proteins identified by coprecipitation from stable or transiently transfected cells (“in vivo” set) and proteins identified by affinity chromatography (“in vitro” set) [14, 15]. Proteins are identified by LocusID numbers or gene symbols, and only those proteins (approximately 80%) with accession numbers annotated in LocusLink are included. Proteins in the in vivo dataset are color coded yellow, and those in the in vitro set are blue, with proteins in common between the two groups in green. The Venn diagram indicates the overlap between the in vivo and in vitro datasets. Prominent clusters are indicated by boxes labeled A-I, and magnified versions of these clusters are shown in Figures S5–S8. Note the coclustering of 14-3-3 binding proteins obtained by distinct approaches within several of these groups.

par genes, of which *par-5* encodes a 14-3-3 protein [34, 35]. By binding to phosphorylated polarity proteins, 14-3-3 isoforms can potentially control their assembly into larger complexes and regulate their polarized subcellular distribution. Consistent with this theme, we identified several polarity determinants, including the PDZ domain scaffolding protein Par-3, its interacting kinase PKC ζ , and the Par-1A kinase [36–38], as well as the cell fate protein Numb-R, in association with 14-3-3 γ [39]. In addition, we found cell junction proteins including Afadin, ZO-2A/TJP2, Plakophilin 2, and p120 catenin, as well as proteins with a polarized subcellular localization; such proteins include Apical Protein of *Xenopus*-Like (APXL), which regulates amiloride-sensitive sodium channel activity [40, 41].

We also identified novel 14-3-3-associated proteins directly involved in regulating actin polymerization and branching through their ability to interact with WAVE isoforms, which in turn bind the Arp2/3 complex. These

include the Nck binding protein NCKAP/NAP125 as well as PIR121 [42]. A NAP125-PIR121-Abi1 complex has been implicated in the activation of WAVE by the Nck SH2/SH3 adaptor and GTP bound Rac [43]. In addition, we identified IRSp53, an adaptor implicated in filopodial formation through interactions with Mena and Cdc42 [44], and also in lamellipodial extensions through association with WAVE and Rac [45]. We also identified a member of the srGAP/WRP family of Rho GTPases, FNB2; we have previously shown that the related WRP/srGAP3 is a Rac GAP that binds through its SH3 domain to WAVE-1 and thereby attenuates Rac-induced actin polymerization [46].

Multiple isoforms of all members of the PAK/Pix/GIT complex were found to associate with 14-3-3 γ (Table 1 and Figure 5A). These proteins have functions in protein trafficking, the formation of focal adhesions, and cell motility [27, 47]. Taken with the identification of multiple Rho GTPase regulators and microtubule-associated

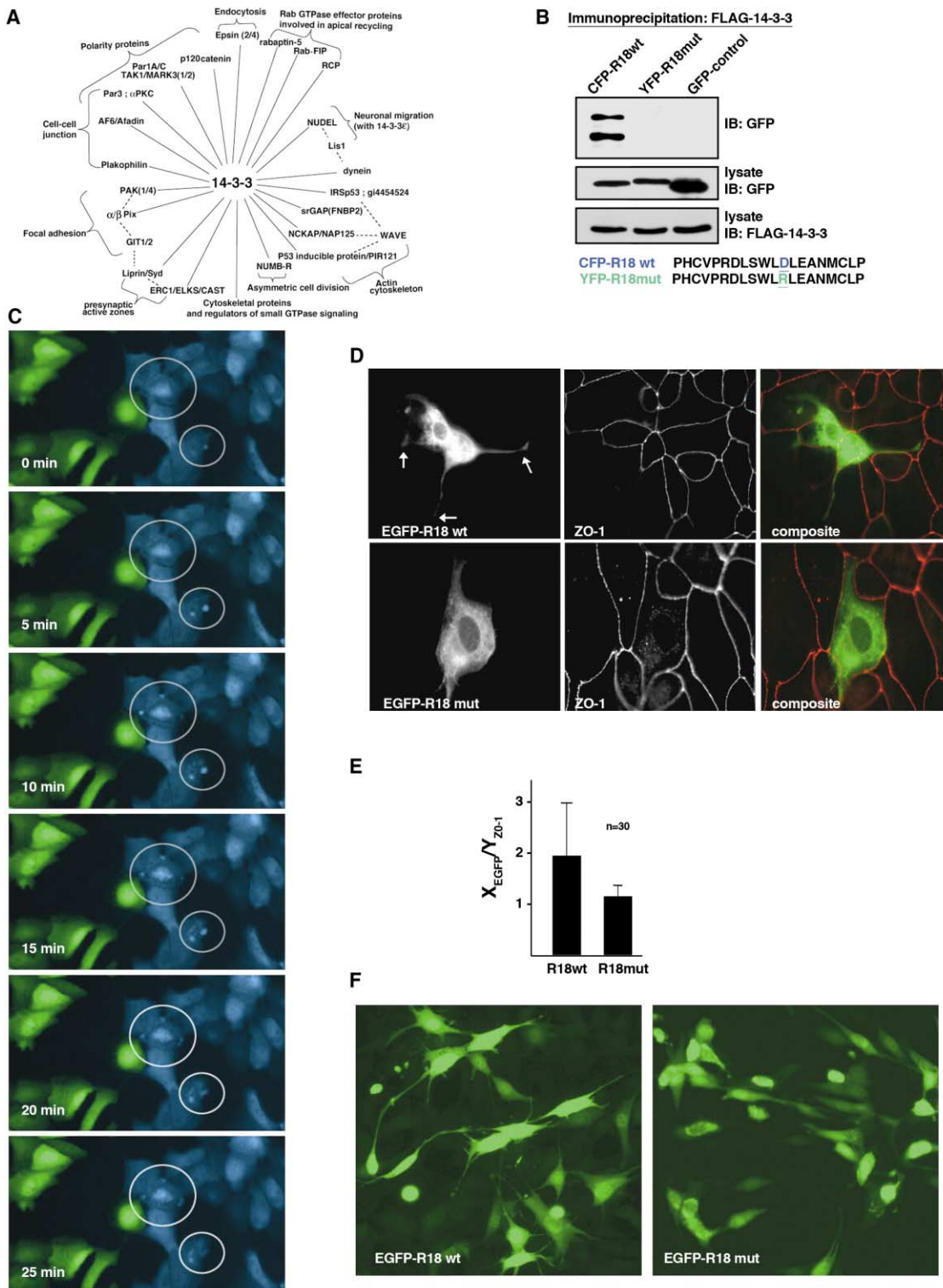


Figure 5. 14-3-3 Phospho-Dependent Interactions Control Dynamic Cell Morphology

(A) 14-3-3 interacting proteins have multiple functions in cytoskeletal regulation and cell fate determination. Solid lines connect 14-3-3 to proteins identified in this study, and dashed lines represent reported interactions. Only a subset of cytoskeletal regulators is shown here (for details, see text and notes in Table 1).

(B) The R18 peptide fused to EGFP fluorescent proteins binds 14-3-3 γ in transfected cells. Flag-14-3-3 γ HEK293 cells were transfected with expression vectors encoding wild-type (WT) or mutant (MUT) R18 peptides fused to ECFP or EYFP respectively, or EGFP alone. The R18MUT sequence has a substitution that converts WLDL to WLRL. Anti-Flag immunoprecipitates were blotted with antibodies to EGFP for detection of R18 fusion proteins (top panel).

proteins, these data indicate that 14-3-3 proteins may play a direct role in multiple facets of cellular architecture (Figure 5A).

In Vivo Inhibition of 14-3-3 Phosphopeptide Binding Modifies Membrane Dynamics and Cell Shape

To explore the role of 14-3-3 proteins in cellular morphology, we examined the effects of blocking 14-3-3 phosphopeptide binding activity in vivo. This was accomplished with a plasmid that encodes the wild-type (WT) R18 peptide fused to enhanced cyan fluorescent protein (ECFP); wild-type R18 peptide antagonizes binding of phosphorylated cellular proteins to 14-3-3 (Figure 5B). As a control, we used an EYFP-fused variant R18 peptide (R18MUT), which no longer binds 14-3-3 because of a substitution (WLRL for WL~~D~~L) in the core motif (Figure 5B). MDCK (Madin-Darby Canine Kidney) epithelial cells in a confluent, polarized monolayer were microinjected with vectors expressing either R18WT-ECFP (Figure 5C, in blue) or R18MUT-EYFP control (Figure 5C, in green) and examined for expression of the fluorescently labeled R18 proteins and for their morphology and migration. The most striking difference between the two groups of cells was that the R18WT cells exhibited enhanced local movement in the form of membrane ruffling and blebbing at the cell periphery, 3 hr after injection. These cells exhibited dynamic and reversible protrusive membrane structures, which were highly fluorescent and suggestive of interaction of the inhibitory R18 peptide with 14-3-3 proteins at these sites (highlighted in Figure 5C; time-lapse video clip Movie 1).

After more prolonged R18WT expression, polarized MDCK cells developed an abnormal morphology, displayed unusual long, branched extensions in comparison to their R18MUT counterparts (Figure 5D), and frequently crawled under their neighbors (image not shown). We quantitated this aberrant cell morphology by measuring the length of a cell's longest horizontal axis (X_{EGFP}), referenced to the diameter of the same cell obtained from cell-cell junction protein ZO-1 (zona occludens 1) staining (Y_{ZO-1}). The ratios of X_{EGFP}/Y_{ZO-1} for cells expressing R18WT and R18MUT peptides (Figure 5E) show that disrupting 14-3-3 phospho-dependent binding had a significant effect ($p < 0.05$) on cell shape. Similar results were obtained with NIH 3T3 fibroblasts (Figure 5F). Of interest, this cytoskeletal remodeling is reminiscent of the effects of vaccinia virus [48], which

can recruit proteins such as Nck, N-WASP, and Arp2/3 to sites of actin assembly through viral gene products [49]. We propose that inhibition of 14-3-3 interactions with associated actin regulatory proteins, such as those identified by proteomic analysis, may underlie the effects of the R18 peptide.

14-3-3 activity does not appear essential for maintaining tight junctions (Figure 5D). However, to assess whether blocking 14-3-3 binding impairs the establishment of these cellular structures, we depolarized the R18-expressing MDCK cells and assessed their ability to reform tight junctions with neighboring cells. Cells with higher levels of R18WT expression failed to form tight junctions with adjacent cells, as indicated by an absence of ZO-1 staining at cell borders, whereas R18MUT was without effect (Figure S9). These experiments suggest that phospho-dependent 14-3-3 interactions are broadly important for cytoskeletal and membrane dynamics and for controlling contact inhibition and the organization of cell junctions.

PKA Suppresses AKAP-Lbc RhoGEF Activity through Phospho-Dependent Binding of 14-3-3 to Ser1565

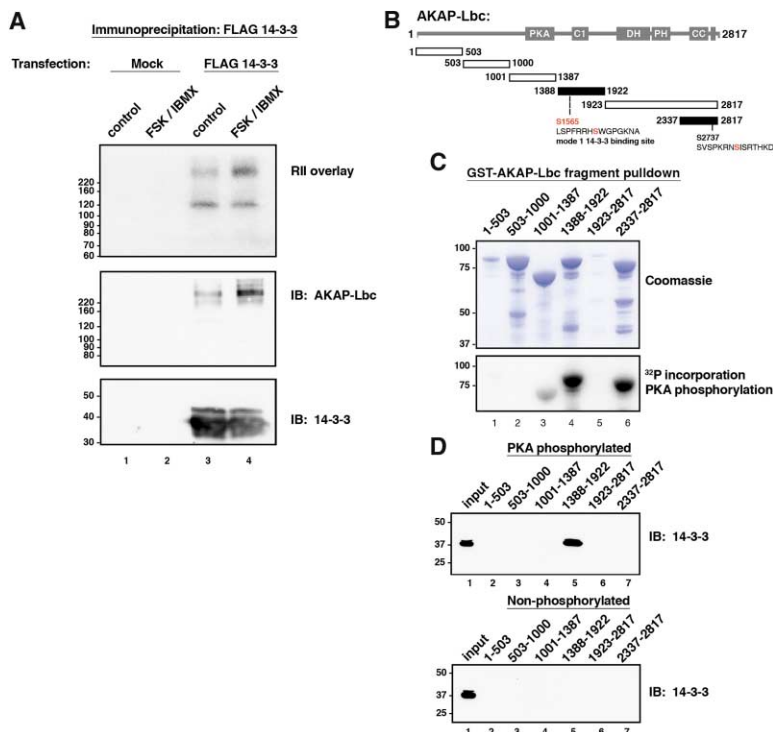
To address more specifically the role 14-3-3 plays in controlling actin dynamics, we sought 14-3-3 targets that can link basophilic protein kinases to the regulation of actin polymerization. PKA (cAMP-dependent protein kinase) has a substrate specificity consistent with phosphorylation of 14-3-3 binding sites. Furthermore, PKA activity is directed to specific substrates through targeting interactions of its regulatory (R) subunits with A kinase anchoring proteins [50–52]. Therefore, we considered the possibility that PKA phosphorylation might promote the recruitment of 14-3-3 to AKAP signaling complexes. We used an RII overlay approach to identify AKAPs that coprecipitated with Flag-14-3-3 γ from HEK293 cells. This technique identified a 14-3-3-associated, RII binding protein of >250 kDa (Figure 6A, upper panel). Binding of the AKAP to 14-3-3 was enhanced upon forskolin/IBMX treatment (compare lanes 3 and 4), suggesting that PKA phosphorylation creates novel 14-3-3 binding sites on this protein. Several AKAPs have a molecular weight in this range, and we therefore attempted to identify the anchoring protein by Western blotting with a panel of AKAP-specific antibodies. A >250 kDa protein that coprecipitated with 14-3-3 γ , in a fashion that was enriched upon PKA activation, was

(C) Fluorescent video microscopy of MDCK cells expressing ECFP-R18. ECFP-R18WT and EYFP-R18MUT plasmids were microinjected into a patch of polarized MDCK cells. After 3 hr, the fluorescent proteins were detected; ECFP-R18WT is shown in blue (right), and EYFP-R18MUT is shown in green (left). Video microscopic images of a fixed viewing field were captured over a period of 25 min and show a dynamic distribution of fluorescently labeled R18 peptide in cells (A full-episode video clip is available as Movie 1). Sites of membrane blebbing induced by R18WT protein are highlighted.

(D) R18-expressing MDCK cells extend aberrant protrusions. Fully polarized MDCK cells were transfected with EGFP-R18WT or EGFP-R18MUT fusion proteins. Twenty-four hours after transfection, cells were fixed and stained for ZO-1 as a marker of cellular tight junctions (red). In contrast to R18MUT-transfected cells, R18WT cells (EGFP, green) showed long protrusions (see arrows), which extended far beyond the ZO-1 cellular margins.

(E) Quantitation of abnormal cell morphologies induced by R18. Thirty randomly selected cells expressing R18WT and 30 cells expressing R18MUT were measured for their longest axis and diameter under EGFP-R18 and ZO-1 filters, respectively. The ratios of these two parameters (X_{EGFP}/Y_{ZO-1}) were plotted as mean values, with error bars representing standard deviations.

(F) NIH 3T3 fibroblasts were transfected with either R18WT-EGFP or R18MUT-EGFP plasmids and imaged for EGFP after 24 hr. R18WT cells show aberrant protrusions.



(C) GST-AKAP-Lbc fusion proteins were purified from bacteria and phosphorylated in vitro with purified PKA catalytic subunit and γ -³²P-ATP. Proteins separated by SDS-PAGE were stained with Coomassie blue (top panel) and exposed to film for determination of ³²P incorporation (bottom panel).

(D) Equivalent amounts of GST-AKAP-Lbc fusion proteins were either phosphorylated in vitro with PKA or left unphosphorylated. Both sets of fusion proteins were then incubated with freshly prepared HEK293 cell lysate for 2 hr at 4°C. After being washed and separated by SDS-PAGE, membranes were probed with pan-14-3-3 antisera. The AKAP-Lbc fragment containing amino acids 1388–1922 binds 14-3-3 upon phosphorylation by PKA (top panel), whereas no binding to any of the fragments is observed when they are not phosphorylated (bottom panel). Input corresponds to 1% of the amount of HEK293 lysate incubated with each fusion protein.

specifically detected with AKAP-Lbc antisera (Figure 6A, middle panel, lanes 3 and 4). In contrast, negative results were obtained when similar filters were probed with antisera against Gravin/AKAP250 or AKAP350/450 (data not shown). Independent confirmation of this result was provided by LC-MS/MS when multiple peptides from AKAP-Lbc were identified in the proteomic analysis of in vivo 14-3-3 γ binding partners (Table 1; Figure S10). AKAP-Lbc clusters with the group of cytoskeletal regulators (Figure 3, green box; Figure 4, box G) because of the presence of a DH-PH RhoGEF cassette, and indeed AKAP-Lbc is a Rho-specific GEF competent for actin regulation [53].

We have recently shown that AKAP-Lbc is phosphorylated by its own pool of anchored PKA [54]. We detected two prominent PKA phosphorylation sites located between residues 1388 and 1922 and residues 2337 and 2817 of AKAP-Lbc by screening GST fusion proteins that encompass overlapping regions of the anchoring protein (Figures 6B and 6C, both panels). In vitro, 14-3-3 bound strongly and selectively to the PKA phosphorylated fragment of AKAP-Lbc containing amino acids 1388–1922 (Figure 6D, lane 5). Control experiments confirmed that 14-3-3 γ did not bind to the non-phosphorylated AKAP-Lbc 1388–1922 fragment (Figure 6D). Scan-site analysis of this region detected one consensus PKA phosphorylation site at serine1565, which interestingly

Figure 6. Phosphorylation-Dependent Interaction of AKAP-Lbc with 14-3-3

(A) HEK293 cells were either mock transfected or transfected with a vector expressing Flag-tagged 14-3-3. Cells were stimulated with either vehicle control or a forskolin/IBMX mix (20 μ M/75 μ M) for 10 min at 37°C. Flag-14-3-3 was immunoprecipitated, and proteins were separated and transferred to nitrocellulose membranes. Membranes were incubated with ³²P-labeled PKA RII subunit to identify RII binding proteins. An RII binding protein >250 kDa was identified (top panel). Binding of this protein to 14-3-3 increased after PKA activation by forskolin/IBMX treatment (lanes 3 and 4). Western blotting with specific antisera identified this protein as AKAP-Lbc (middle panel). Blotting with 14-3-3 antisera confirmed the presence of 14-3-3 in Flag immunoprecipitates but not in immunoprecipitates from mock-transfected cells (bottom panel).

(B) Schematic diagram of AKAP-Lbc showing the regions of the protein that were expressed as GST fusion proteins in bacteria. The PKA binding site (PKA) and C1, DH-PH (RhoGEF), and coiled-coil (CC) domains are indicated. Two potential PKA phosphorylation sites as determined by Scansite analysis are shown. The first site, serine1565, also falls within a predicted mode 1 14-3-3 binding site.

was located within a putative mode 1 14-3-3 binding site (Figure 6B). Site-directed mutagenesis studies demonstrated that substitution of serine1565 by alanine significantly reduced PKA phosphorylation of the AKAP-Lbc 1388–1922 fragment (Figure 7A, lane 3) when compared to the wild-type fragment (Figure 7A, lane 2). This suggests that Ser1565 is the principal PKA phosphorylation site in this region of AKAP-Lbc. In vitro binding studies demonstrated that a GST fusion of AKAP-Lbc residues 1388–1922 was unable to bind 14-3-3 after preincubation with PKA when Ser1565 was mutated to Ala (Figure 7B).

Wild-type (WT) or mutant AKAP-Lbc proteins were then expressed and immunoprecipitated from HEK293 or COS-7 cells, and immune complexes were blotted for 14-3-3. The S1565A mutation strongly reduced both basal and forskolin/IBMX-induced 14-3-3 interaction with AKAP-Lbc (Figure 7C). Collectively, these data identify Ser1565 of AKAP-Lbc as a specific phosphorylation-dependent 14-3-3 binding site, modified by PKA in vivo.

To investigate whether phosphorylation of Ser1565 may regulate the RhoGEF activity of AKAP-Lbc, we used two complementary assays to analyze the effect of the S1565A mutation on the ability of full-length AKAP-Lbc to stimulate GTP bound Rho in vivo. In one approach, we employed a FRET (fluorescent resonance energy transfer)-based technique to specifically measure the

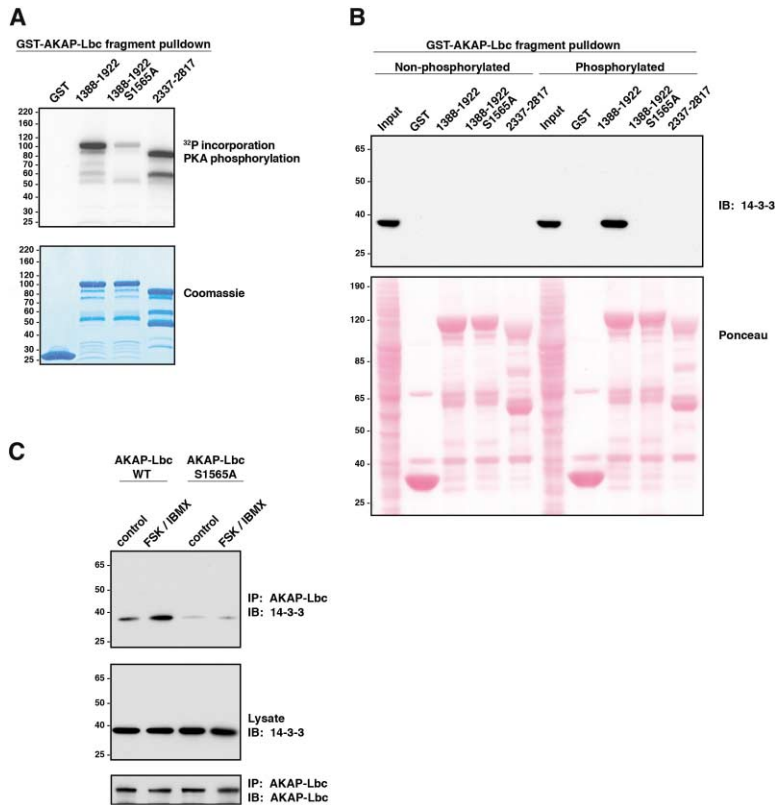


Figure 7. PKA Phosphorylation of AKAP-Lbc Ser1565 Mediates 14-3-3 Binding.

(A) Serine 1565 in GST-AKAP-Lbc 1388–1922 was mutated to alanine and expressed in bacteria. GST fusion proteins were phosphorylated *in vitro* by PKA as described. Proteins separated by SDS-PAGE were stained with Coomassie blue (bottom panel) and exposed to film for determination of ³²P incorporation (top panel). Mutation of S1565 to alanine largely abolished PKA phosphorylation of this fusion protein, indicating this residue is the major site of PKA phosphorylation in this region of AKAP-Lbc (top panel).

(B) GST-AKAP-Lbc 1388–1922 and GST-AKAP-Lbc 1388–1922 S1565A were phosphorylated *in vitro* by PKA or left unphosphorylated. Fusion proteins were then incubated with HEK293 cell lysate for 2 hr at 4°C. After washing and SDS-PAGE, membranes were Western blotted for 14-3-3 (top panel). Mutation of serine 1565 to alanine abolishes PKA phosphorylation-induced binding of GST-AKAP-Lbc 1388–1922 to 14-3-3. GST and GST-AKAP-Lbc 2337–2817 were used as controls. Input represents 1% of the HEK293 lysate added to the fusion proteins. Ponceau staining demonstrates equal loading of fusion proteins (bottom panel).

(C) Flag-tagged full-length AKAP-Lbc WT or AKAP-Lbc S1565A cDNAs expressed in COS-7 cells. Cells were treated with vehicle or with forskolin/IBMX (20 μM/75 μM) for 10 min at 37°C. Flag-agarose was used for immunopurification of AKAP-Lbc proteins from lysates. After SDS-PAGE and transfer, membranes were probed with pan-14-3-3 antisera. Forskolin/IBMX treatment increases the amount of 14-3-3 associated with wild-type AKAP-Lbc. Mutation of serine1565 to alanine reduces basal 14-3-3 binding and abolishes forskolin/IBMX-induced AKAP-Lbc-14-3-3 interactions (top panel). Equivalent amounts of 14-3-3 in the lysates (middle panel) and precipitated AKAP-Lbc proteins (bottom panel) were confirmed by Western blotting.

ification of AKAP-Lbc proteins from lysates. After SDS-PAGE and transfer, membranes were probed with pan-14-3-3 antisera. Forskolin/IBMX treatment increases the amount of 14-3-3 associated with wild-type AKAP-Lbc. Mutation of serine1565 to alanine reduces basal 14-3-3 binding and abolishes forskolin/IBMX-induced AKAP-Lbc-14-3-3 interactions (top panel). Equivalent amounts of 14-3-3 in the lysates (middle panel) and precipitated AKAP-Lbc proteins (bottom panel) were confirmed by Western blotting.

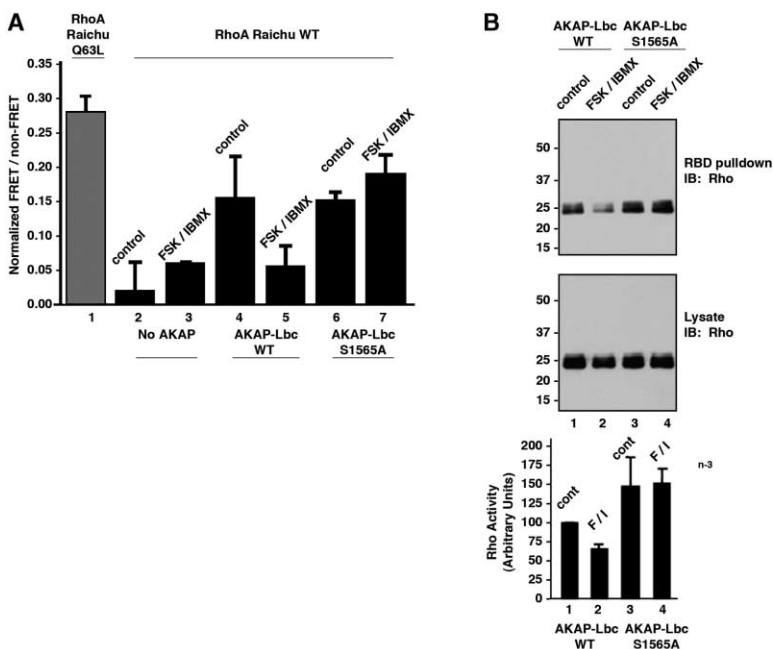
ratio of active GTP bound RhoA to inactive GDP bound RhoA by using NIH 3T3 cells transfected with WT AKAP-Lbc or the S1565A mutant. We measured the state of Rho activation by using a RhoA-Raichu probe [55] that contains the Rho GTPase joined to the Rho-GTP binding domain of PKN, with yellow fluorescence protein (YFP) and cyan fluorescence protein (CFP) fused to the N- or C termini, respectively. When the RhoA component of the RhoA-Raichu chimera is bound to GTP, it associates with the linked GTPase binding domain and thereby juxtaposes YFP and CFP such that they undergo FRET. Both the WT and S1565A mutant forms of AKAP-Lbc stimulated RhoA GTP loading in control cells treated only with the phosphodiesterase inhibitor IBMX (Figure 8A). However, upon treatment with both forskolin and IBMX to elevate cAMP and activate PKA, WT AKAP-Lbc no longer induced RhoA activation (Figure 8A, column 5). In contrast, the S1565A mutant of AKAP-Lbc retained full RhoGEF activity in the presence of forskolin/IBMX (Figure 8A, column 7; consistent results were obtained in three separate experiments).

In complementary experiments, we used a GST-Rho-tekkin fusion, which selectively binds Rho-GTP, to monitor the extent of Rho activation in COS-7 cells expressing WT or mutant AKAP-Lbc by using a pull-down assay. Once again, we found that forskolin/IBMX stimulation of cells transfected with WT AKAP-Lbc suppressed the level of Rho-GTP by approximately 35% (Figure 8B, lane

2), whereas the S1565A mutant was unaffected by elevated cAMP and attendant PKA activation (Figure 8B). In both sets of experiments, the expression of WT and S1565A mutant proteins was equivalent (data not shown). These findings are consistent with a model in which cAMP activates a pool of PKA anchored to AKAP-Lbc to catalyze the phosphorylation of Ser 1565. The concomitant recruitment of 14-3-3 suppresses AKAP-Lbc RhoGEF activity. This scheme provides a molecular explanation for evidence that cAMP-responsive events attenuate Rho activation [51]. Furthermore, this pathway provides a direct means to link PKA activity to RhoA and the formation of actin stress fibers through the 14-3-3-mediated control of AKAP-Lbc.

Conclusion

We have used tandem proteomic and biochemical techniques to identify polypeptides that are associated with 14-3-3 proteins *in vivo*. These approaches provide an important, physiological counterpart to the analysis of 14-3-3 binding proteins by *in vitro* affinity chromatography and have revealed a distinct spectrum of 14-3-3 binding proteins. Our data have uncovered a broad range of 14-3-3-associated proteins with numerous potential functions. In order to understand and exploit this large amount of information, we have devised a domain-based clustering approach to analyze this relatively significant fraction of the proteome. This technique defines



lized GST-RBD for 1 hr at 4°C. After extensive washing, bound proteins were separated by SDS-PAGE, and blots were probed with anti-HA antisera. Forskolin/IBMX treatment results in an inhibition of WT AKAP-Lbc GEF activity and decreased Rho-GTP (top panel). This effect is abolished upon serine 1565 mutation to alanine in the PKA phosphorylation/14-3-3 binding site (top panel). Rho-GTP levels were normalized to total Rho present in cell lysates (middle panel) and quantified by densitometry (bottom panel).

Figure 8. Phosphorylation of Ser1565 Suppresses AKAP-Lbc RhoGEF Activity against RhoA

(A) The fraction of GTP bound RhoA-Raichu was measured in NIH 3T3 cells. NIH 3T3 cells were transiently cotransfected with the Raichu plasmids containing activated (Q63L) or wild-type (WT) RhoA, together with AKAP-Lbc expression vectors (WT, S1565A) as indicated. The cells were then serum starved for 24 hr, followed by addition of IBMX (control) or both IBMX and forskolin (FSK/IBMX). Ten minutes later, cells were lysed, and fluorescence emission spectra from the lysates were subsequently collected. Each bar represents the averaged normalized ratio of fluorescence at 528 nm (FRET) over 480 nm (non-FRET) from two separate transfections with their standard deviation.

(B) RhoA activity of WT AKAP-Lbc and AKAP-Lbc S1565A was measured with rhotekin RBD pulldowns. COS-7 cells transfected with vectors expressing HA-RhoA and either AKAP-Lbc or AKAP-Lbc S1565A were serum starved for 6 hr and treated with vehicle or forskolin/IBMX (20 μM/75 μM) for 10 min at 37°C. Cleared lysates were incubated with immobi-

specific subsets of structurally related 14-3-3 interacting proteins, which are thereby implicated in common aspects of cellular regulation. We propose that this computational approach will be of general utility in the analysis of large protein datasets.

A notable feature of 14-3-3 binding proteins revealed by this procedure is their involvement in regulation of the cytoskeleton, GTPase function, membrane signaling, and cell fate determination. The significance of these proteomic data is supported by the effects of inhibiting 14-3-3 phosphopeptide binding in living cells, which leads to markedly altered membrane dynamics, cell protrusions, and ability to establish tight junctions. In pursuit of scaffolding proteins that might physically link 14-3-3 to both a basophilic kinase and actin regulation, we have distinguished AKAP-Lbc as an *in vivo* 14-3-3 binding protein. We identified AKAP-Lbc as a protein that can bind both to the RII regulatory subunit of PKA, as well as to 14-3-3 through a specific pSer motif modified by PKA. Phospho-dependent binding of 14-3-3 to AKAP-Lbc suppresses its ability to activate Rho, a GTPase that regulates the formation of actin stress fibers. Such inhibition might be achieved through a variety of mechanisms, such as locking the DH domain of AKAP-Lbc in an inactive conformation or interfering with its access to Rho. AKAP-Lbc is therefore well positioned to contribute to the effects of 14-3-3 on the actin cytoskeleton.

In preliminary proteomic experiments, we have found that 14-3-3 interactions can be used as a probe to distinguish between the activation of different cellular signaling pathways (J.J., unpublished data). Because 14-3-3 proteins sample a wide subset of the phosphoproteome, mass spectrometry techniques for the quantitative anal-

ysis of differential protein complexes could be exploited as a means to explore the extent of 14-3-3 interactions, and thus protein phosphorylation, under different physiological or pathological conditions.

Supplemental Data

Supplemental Experimental Procedures, a movie, three tables, and ten supplemental figures are available with this article online at <http://www.current-biology.com/cgi/content/full/14/16/1436/DC1/>.

Acknowledgments

We acknowledge Robert Steven, Karen Colwill, and Yinon Ben-Neriah for technical suggestions and advice and Michiyuki Matsuda for the RhoA-Raichu probe. The work was supported by grants from Genome Canada and the Canadian Institutes for Health Research to T.P.. Additionally, J.D.S. was supported by the Howard Hughes Medical Institute and the National Institutes of Health (grant number DK44239). T.P. is a Distinguished Scientist of the Canadian Institutes for Health Research. T.P. is a consultant for MDS-Proteomics.

Received: June 25, 2004

Revised: July 14, 2004

Accepted: July 14, 2004

Published online: July 22, 2004

References

- Hunter, T. (2000). Signaling—2000 and beyond. *Cell* 100, 113–127.
- Pawson, T., and Nash, P. (2003). Assembly of cell regulatory systems through protein interaction domains. *Science* 300, 445–452.
- Muslin, A.J., Tanner, J.W., Allen, P.M., and Shaw, A.S. (1996). Interaction of 14-3-3 with signaling proteins is mediated by the recognition of phosphoserine. *Cell* 84, 889–897.
- Yaffe, M.B., Rittinger, K., Volinia, S., Caron, P.R., Aitken, A., Leffers, H., Gamblin, S.J., Smerdon, S.J., and Cantley, L.C.

- (1997). The structural basis for 14-3-3:phosphopeptide binding specificity. *Cell* 91, 961-971.
5. Obsil, T., Ghirlando, R., Klein, D.C., Ganguly, S., and Dyda, F. (2001). Crystal structure of the 14-3-3:serotonin N-acetyltransferase complex. a role for scaffolding in enzyme regulation. *Cell* 105, 257-267.
 6. Fu, H., Subramanian, R.R., and Masters, S.C. (2000). 14-3-3 proteins: structure, function, and regulation. *Annu. Rev. Pharmacol. Toxicol.* 40, 617-647.
 7. Yaffe, M.B. (2002). How do 14-3-3 proteins work?—Gatekeeper phosphorylation and the molecular anvil hypothesis. *FEBS Lett.* 513, 53-57.
 8. Pozuelo Rubio, M., Peggie, M., Wong, B.H., Morrice, N., and MacKintosh, C. (2003). 14-3-3s regulate fructose-2,6-bisphosphate levels by binding to PKB-phosphorylated cardiac fructose-2,6-bisphosphate kinase/phosphatase. *EMBO J.* 22, 3514-3523.
 9. Benton, R., Palacios, I.M., and St Johnston, D. (2002). *Drosophila* 14-3-3/Par-5 is an essential mediator of PAR-1 function in axis formation. *Dev. Cell* 3, 659-671.
 10. MacKintosh, C. (2004). Dynamic interactions between 14-3-3s and phosphoproteins regulate diverse cellular processes. *Biochem. J.* 381, 329-342.
 11. Hermeking, H. (2003). The 14-3-3 cancer connection. *Nat. Rev. Cancer* 3, 931-943.
 12. Datta, S.R., Dudek, H., Tao, X., Masters, S., Fu, H., Gotoh, Y., and Greenberg, M.E. (1997). Akt phosphorylation of BAD couples survival signals to the cell-intrinsic death machinery. *Cell* 91, 231-241.
 13. Brunet, A., Bonni, A., Zigmond, M.J., Lin, M.Z., Juo, P., Hu, L.S., Anderson, M.J., Arden, K.C., Blenis, J., and Greenberg, M.E. (1999). Akt promotes cell survival by phosphorylating and inhibiting a Forkhead transcription factor. *Cell* 96, 857-868.
 14. Rubio, M.P., Geraghty, K.M., Wong, B.H., Wood, N.T., Campbell, D.G., Morrice, N., and Mackintosh, C. (2004). 14-3-3-affinity purification of over 200 human phosphoproteins reveals new links to regulation of cellular metabolism, proliferation and trafficking. *Biochem. J.* 379, 395-408.
 15. Meek, S.E., Lane, W.S., and Piwnicka-Worms, H. (2004). Comprehensive proteomic analysis of interphase and mitotic 14-3-3 binding proteins. *J. Biol. Chem.* Published online June 4. 10.1074/jbc.M403044200.
 16. Chaudhri, M., Scarabel, M., and Aitken, A. (2003). Mammalian and yeast 14-3-3 isoforms form distinct patterns of dimers in vivo. *Biochem. Biophys. Res. Commun.* 300, 679-685.
 17. Wang, B., Yang, H., Liu, Y.C., Jelinek, T., Zhang, L., Ruoslahti, E., and Fu, H. (1999). Isolation of high-affinity peptide antagonists of 14-3-3 proteins by phage display. *Biochemistry* 38, 12499-12504.
 18. Petosa, C., Masters, S.C., Bankston, L.A., Pohl, J., Wang, B., Fu, H., and Liddington, R.C. (1998). 14-3-3zeta binds a phosphorylated Raf peptide and an unphosphorylated peptide via its conserved amphipathic groove. *J. Biol. Chem.* 273, 16305-16310.
 19. Gene Ontology Consortium. (2001). Creating the gene ontology resource: design and implementation. *Genome Res.* 11, 1425-1433.
 20. Obenauer, J.C., Cantley, L.C., and Yaffe, M.B. (2003). Scansite 2.0: proteome-wide prediction of cell signaling interactions using short sequence motifs. *Nucleic Acids Res.* 31, 3635-3641.
 21. Eisen, M.B., Spellman, P.T., Brown, P.O., and Botstein, D. (1998). Cluster analysis and display of genome-wide expression patterns. *Proc. Natl. Acad. Sci. USA* 95, 14863-14868.
 22. Wilson, M.I., Gill, D.J., Perisic, O., Quinn, M.T., and Williams, R.L. (2003). PB1 domain-mediated heterodimerization in NADPH oxidase and signaling complexes of atypical protein kinase C with Par6 and p62. *Mol. Cell* 12, 39-50.
 23. Nakamura, K., and Johnson, G.L. (2003). PB1 domains of MEKK2 and MEKK3 interact with the MEK5 PB1 domain for activation of the ERK5 pathway. *J. Biol. Chem.* 278, 36989-36992.
 24. Lin, D., Edwards, A.S., Fawcett, J.P., Mbamalu, G., Scott, J.D., and Pawson, T. (2000). A mammalian PAR-3-PAR-6 complex implicated in Cdc42/Rac1 and aPKC signalling and cell polarity. *Nat. Cell Biol.* 2, 540-547.
 25. Joberty, G., Petersen, C., Gao, L., and Macara, I.G. (2000). The cell-polarity protein Par6 links Par3 and atypical protein kinase C to Cdc42. *Nat. Cell Biol.* 2, 531-539.
 26. Nassar, N., Horn, G., Herrmann, C., Scherer, A., McCormick, F., and Wittinghofer, A. (1995). The 2.2 Å crystal structure of the Ras-binding domain of the serine/threonine kinase c-Raf1 in complex with Rap1A and a GTP analogue. *Nature* 375, 554-560.
 27. Bokoch, G.M. (2003). Biology of the p21-activated kinases. *Annu. Rev. Biochem.* 72, 743-781.
 28. Motoyama, N., and Naka, K. (2004). DNA damage tumor suppressor genes and genomic instability. *Curr. Opin. Genet. Dev.* 14, 11-16.
 29. Mayor, T., Hacker, U., Stierhof, Y.D., and Nigg, E.A. (2002). The mechanism regulating the dissociation of the centrosomal protein C-Nap1 from mitotic spindle poles. *J. Cell Sci.* 115, 3275-3284.
 30. Kisseleva, M.V., Wilson, M.P., and Majerus, P.W. (2000). The isolation and characterization of a cDNA encoding phospholipid-specific inositol polyphosphate 5-phosphatase. *J. Biol. Chem.* 275, 20110-20116.
 31. Guimera, J., Casas, C., Estivill, X., and Pritchard, M. (1999). Human minibrain homologue (MNBH/DYRK1): characterization, alternative splicing, differential tissue expression, and overexpression in Down syndrome. *Genomics* 57, 407-418.
 32. Altafaj, X., Dierssen, M., Baamonde, C., Marti, E., Visa, J., Guimera, J., Oset, M., Gonzalez, J.R., Florez, J., Fillat, C., et al. (2001). Neurodevelopmental delay, motor abnormalities and cognitive deficits in transgenic mice overexpressing Dyrk1A (minibrain), a murine model of Down's syndrome. *Hum. Mol. Genet.* 10, 1915-1923.
 33. Wilson, F.H., Disse-Nicodeme, S., Choate, K.A., Ishikawa, K., Nelson-Williams, C., Desitter, I., Gunel, M., Milford, D.V., Lipkin, G.W., Achard, J.M., et al. (2001). Human hypertension caused by mutations in WNK kinases. *Science* 293, 1107-1112.
 34. Macara, I.G. (2004). Par proteins: partners in polarization. *Curr. Biol.* 14, R160-R162.
 35. Kempfues, K. (2000). PARSing embryonic polarity. *Cell* 101, 345-348.
 36. Benton, R., and St Johnston, D. (2003). *Drosophila* PAR-1 and 14-3-3 inhibit Bazooka/PAR-3 to establish complementary cortical domains in polarized cells. *Cell* 115, 691-704.
 37. Hurd, T.W., Fan, S., Liu, C.J., Kweon, H.K., Hakansson, K., and Margolis, B. (2003). Phosphorylation-dependent binding of 14-3-3 to the polarity protein Par3 regulates cell polarity in mammalian epithelia. *Curr. Biol.* 13, 2082-2090.
 38. Brajenovic, M., Joberty, G., Kuster, B., Bouwmeester, T., and Drewes, G. (2004). Comprehensive proteomic analysis of human Par protein complexes reveals an interconnected protein network. *J. Biol. Chem.* 279, 12804-12811.
 39. Petersen, P.H., Zou, K., Hwang, J.K., Jan, Y.N., and Zhong, W. (2002). Progenitor cell maintenance requires numb and numb-like during mouse neurogenesis. *Nature* 419, 929-934.
 40. Schiaffino, M.V., Bassi, M.T., Rugarli, E.I., Renieri, A., Galli, L., and Ballabio, A. (1995). Cloning of a human homologue of the *Xenopus laevis* APX gene from the ocular albinism type 1 critical region. *Hum. Mol. Genet.* 4, 373-382.
 41. Raychowdhury, M.K., Ibarra, C., Damiano, A., Jackson, G.R., Jr., Smith, P.R., McLaughlin, M., Prat, A.G., Ausiello, D.A., Lader, A.S., and Cantiello, H.F. (2004). Characterization of Na⁺-permeable cation channels in LLC-PK1 renal epithelial cells. *J. Biol. Chem.* 279, 20137-20146.
 42. Eden, S., Rohatgi, R., Podtelejnikov, A.V., Mann, M., and Kirschner, M.W. (2002). Mechanism of regulation of WAVE1-induced actin nucleation by Rac1 and Nck. *Nature* 418, 790-793.
 43. Innocenti, M., Zucconi, A., Disanza, A., Frittoli, E., Arecas, L.B., Steffen, A., Stradal, T.E., Di Fiore, P.P., Carlier, M.F., and Scita, G. (2004). Abi1 is essential for the formation and activation of a WAVE2 signaling complex. *Nat. Cell Biol.* 6, 319-327.
 44. Krugmann, S., Jordens, I., Gevaert, K., Driessens, M., Vandekerckhove, J., and Hall, A. (2001). Cdc42 induces filopodia by promoting the formation of an IRSp53:Mena complex. *Curr. Biol.* 11, 1645-1655.

45. Miki, H., Yamaguchi, H., Suetsugu, S., and Takenawa, T. (2000). IRSp53 is an essential intermediate between Rac and WAVE in the regulation of membrane ruffling. *Nature* *408*, 732–735.
46. Soderling, S.H., Binns, K.L., Wayman, G.A., Davee, S.M., Ong, S.H., Pawson, T., and Scott, J.D. (2002). The WRP component of the WAVE-1 complex attenuates Rac-mediated signalling. *Nat. Cell Biol.* *4*, 970–975.
47. Webb, D.J., Brown, C.M., and Horwitz, A.F. (2003). Illuminating adhesion complexes in migrating cells: moving toward a bright future. *Curr. Opin. Cell Biol.* *15*, 614–620.
48. Sanderson, C.M., Way, M., and Smith, G.L. (1998). Virus-induced cell motility. *J. Virol.* *72*, 1235–1243.
49. Smith, G.L., Murphy, B.J., and Law, M. (2003). Vaccinia virus motility. *Annu. Rev. Microbiol.* *57*, 323–342.
50. Michel, J.J., and Scott, J.D. (2002). AKAP mediated signal transduction. *Annu. Rev. Pharmacol. Toxicol.* *42*, 235–257.
51. Diviani, D., and Scott, J.D. (2001). AKAP signaling complexes at the cytoskeleton. *J. Cell Sci.* *114*, 1431–1437.
52. Alto, N.M., Soderling, S.H., Hoshi, N., Langeberg, L.K., Fayos, R., Jennings, P.A., and Scott, J.D. (2003). Bioinformatic design of A-kinase anchoring protein-in silico: a potent and selective peptide antagonist of type II protein kinase A anchoring. *Proc. Natl. Acad. Sci. USA* *100*, 4445–4450.
53. Diviani, D., Soderling, J., and Scott, J.D. (2001). AKAP-Lbc anchors protein kinase A and nucleates Galpha 12-selective Rho-mediated stress fiber formation. *J. Biol. Chem.* *276*, 44247–44257.
54. Carnegie, G.K., Smith, F.D., McConnachie, G., Langeberg, L.K., and Scott, J.D. (2004). AKAP-Lbc nucleates a protein kinase D activation scaffold. *Mol. Cell*, in press.
55. Itoh, R.E., Kurokawa, K., Ohba, Y., Yoshizaki, H., Mochizuki, N., and Matsuda, M. (2002). Activation of rac and cdc42 video imaged by fluorescent resonance energy transfer-based single-molecule probes in the membrane of living cells. *Mol. Cell. Biol.* *22*, 6582–6591.